

INFLUENCE OF ABRASIVE WEAR MODES ON THE COEFFICIENT OF FRICTION OF THIN FILMS

Ronaldo Câmara Cozza^{1,2}

Jorge Thiago de Sousa Lima Wilcken¹

Cláudio Geraldo Schön³

Abstract

The purpose of this work is to study the influence of abrasive wear modes on the coefficient of friction (μ) of thin films. Initially, free rotative-ball micro-abrasive wear testing equipment was designed and constructed to measure the coefficient of friction on the tribological system “thin film – abrasive slurry – test sphere”. Experiments were conducted with thin films of TiN, CrN, TiAlN, ZrN, TiZrN, TiN/TiAlN, TiN/TiAlN (multi-layer), TiHfC and TiHfCN using a ball of AISI 52100 steel and abrasive slurries prepared with black silicon carbide (SiC) particles and glycerine. The aim of this design was to produce “*grooving abrasion*” and “*rolling abrasion*” on the surface of thin films. The normal force (N) and the tangential force (T) were monitored throughout the tests, and the coefficient of friction was calculated as $\mu = T/N$. Aside from the thin film type, e.g., for all thin films studied, the results that have been obtained in this work show that the abrasive slurry concentration affected the abrasive wear modes (“*grooving abrasion*” or “*rolling abrasion*”) and, consequently, the magnitude of the coefficient of friction: *i*) a low abrasive slurry concentration was related with grooving abrasion and a relatively high coefficient of friction; *ii*) a high abrasive slurry concentration was related with rolling abrasion and a relatively low coefficient of friction.

Keywords: Abrasion; Grooving abrasion; Rolling abrasion; Thin films; Coefficient of friction.

1 INTRODUCTION

The micro-abrasive wear test by rotative ball is an important method adopted to study the abrasive wear behaviour of materials. Figure 1 presents a schematic diagram of the principle of this abrasive wear test in which a rotating ball is forced against the tested specimen in the presence of an abrasive slurry.

Initially, the development of the ball-cratering wear test aimed to measure the thickness of thin films [1] (Figures 2a and 2b). However, because of the technical features, this type of abrasive wear test has been applied to study the wear volume (V), coefficient of wear (k) and coefficient of friction (μ) of different materials, such as metallic, polymeric and ceramic materials [2-5].

In the analysis of tribological behavior of thin films, it is possible to calculate their wear volume, coefficient of wear and coefficient of friction [2,6-10] using Equations 1-7 detailed below, from Reference [2].

With the value of the crater depth (h) and from Equation 1, the total wear volume (V) (coating and substrate – Figure 2c) can be calculated. “ R ” is the radius of the test sphere

and the dimension “ h ” (total depth of the wear crater) is schematized in Figure 1.

$$V \cong \pi R h^2 \text{ for } h \ll R \quad (1)$$

The wear volume of the substrate (V_s) and the wear volume of the coating (V_c) can be calculated from Equations 2 and 3, respectively; “ h_c ” is the coating thickness (Figure 2d).

$$V_s \cong \pi R (h - h_c)^2 \text{ for } h \ll R \quad (2)$$

$$V_c \cong \pi R (2h h_c - h_c^2) \text{ for } h \ll R \quad (3)$$

The total wear coefficient (k_t), the wear coefficient of the substrate (k_s) and the wear coefficient of the coating (k_c) can be calculated from Equations 4, 5 and 6, respectively. In Figure 2e, “ a ” is the internal crater diameter and “ b ” is the external crater diameter [11]. “ N ” is the normal force and “ S ” is the sliding distance.

$$k_t = \frac{\pi R h^2}{NS} \quad (4)$$

¹Departamento de Engenharia Mecânica, Centro Universitário, Fundação Educacional Inaciana “Padre Sabóia de Medeiros” – FEI, São Bernardo do Campo, SP, Brasil. E-mail: rcamara@fei.edu.br; ronaldo.cozza@fatec.sp.gov.br

²Departamento de Fabricação Mecânica, Centro Estadual de Educação Tecnológica “Paula Souza” – CEETEPS, Faculdade de Tecnologia – FATEC-Mauá, Mauá, SP, Brasil.

³Departamento de Engenharia Metalúrgica e de Materiais, Escola Politécnica, Universidade de São Paulo – USP, São Paulo, SP, Brasil.



$$k_s = \frac{\pi R(h - h_c)^2}{NS}$$

$$k_c = \frac{\pi R(2hh_c - h_c^2)}{NS}$$

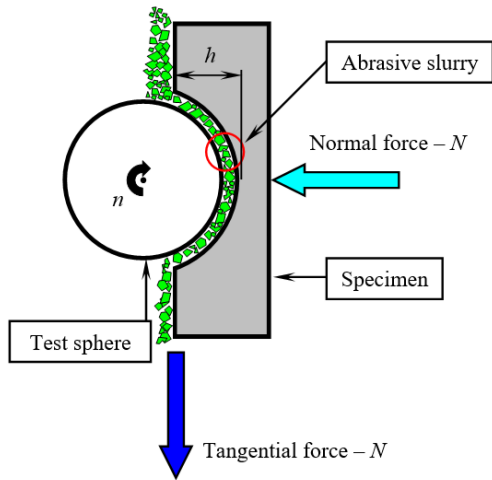


Figure 1. Micro-abrasive wear test by rotating ball: A representative figure showing the operating principle and the abrasive particles between the test sphere and the specimen; “*h*” is the depth of the wear crater and “*n*” is the test sphere rotational speed.

(5) Completing the thin films analysis carried out by Cozza [2], the coefficient of friction acting on the tribological system “specimen – abrasive particles – test sphere” has been calculated by Equation 7:

(6)
$$\mu = \frac{T}{N}$$
 (7)

In the micro-abrasive wear test by rotative ball, the “wear craters” that are generated on the specimen can present two abrasive wear modes, which are observed on the surface of the worn crater: “*grooving abrasion*” is observed when the abrasive particles slide on the surface, whereas “*rolling abrasion*” results from abrasive particles rolling on the specimen.

Figures 3a [3, 12] and 3b present, respectively, images of “*grooving abrasion*” and “*rolling abrasion*”. Figure 3a refers to a ball-cratering abrasive wear test conducted with an AISI H10 tool-steel specimen, under the following test conditions: normal force $N = 1.25$ N, abrasive slurry concentration $C = 25\%$ SiC + 75% distilled water (in volume) and test sphere rotational speed $n = 37.6$ rpm; Figure 3b refers to a ball-cratering abrasive wear test conducted with a specimen of Fe-30Al-6Cr (at.%) iron aluminide alloy [4], under the following test conditions: normal force $N = 0.25$ N, abrasive slurry concentration $C = 50\%$ SiC + 50% glycerin (in volume) and test sphere rotational speed $n = 37.6$ rpm.

Many works on coefficient of friction (μ) during abrasive wear and other types of tests are available in the literature [13-15], but only a few were dedicated to the coefficient of friction

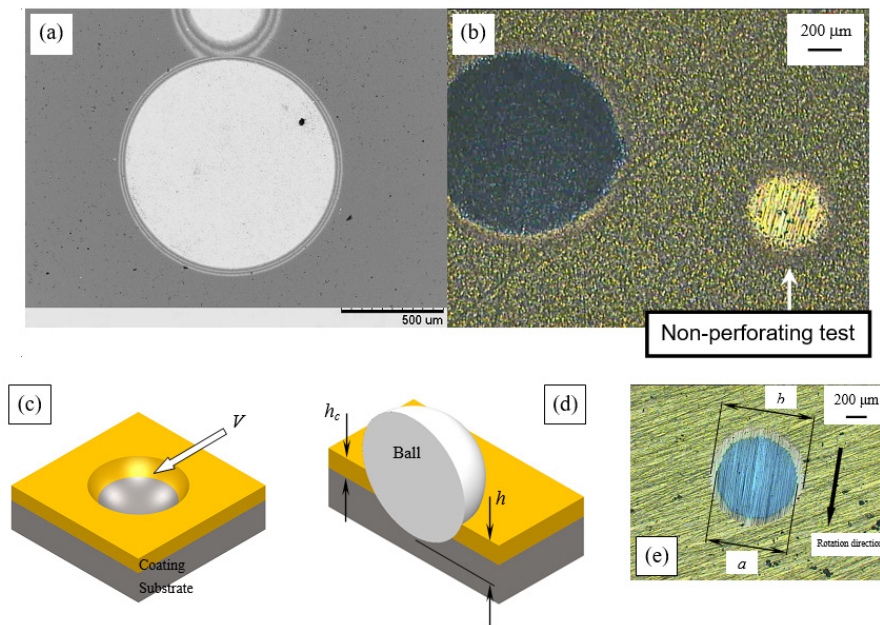


Figure 2. Examples of wear craters generated on coated systems: (a) multi-layer, (b) thin film of TiN (crater of right: non-perforating test, e.g., without reaching the substrate), (c) total wear volume – “*V*” (schematic illustration), (d) total crater depth – “*h*” and coating thickness – “*h_c*” (schematic illustration), (e) internal diameter – “*a*” and external diameter – “*b*” [11].

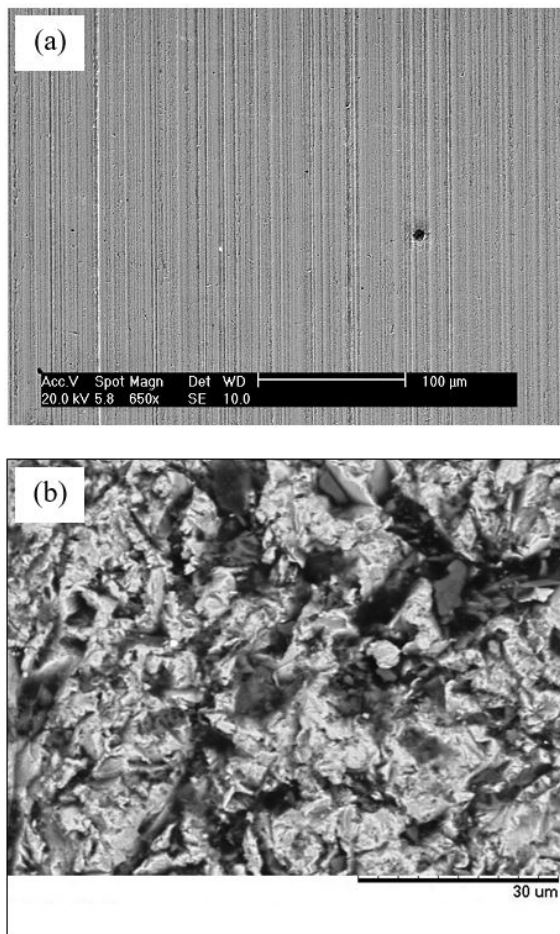


Figure 3. Abrasive wear modes: (a) “grooving abrasion” [3,12] and (b) “rolling abrasion”.

in ball-cratering wear tests [2-4,10,12,16,17]. In particular, Shipway [16] has studied the coefficient of friction in terms of the shape and movement of the abrasive particles, Kusano and Hutchings [17] presented a theoretical model for coefficient of friction in micro-abrasive wear tests with free ball equipment configuration and Cozza et al. [2-4,11,18] measured the tangential force developed during tests conducted in a fixed ball equipment configuration, which allowed direct calculation of the friction coefficient by the ratio between the tangential and normal forces. Besides, using a proper electronic instrumentation, Cozza et al. [2,11,19-22] have studied and measured the behaviour of the coefficient of friction in thin films in ball-cratering wear tests; however, in those works [2,11,19-22], the test sphere has reached the substrate.

With the intent to collaborate with the understanding of the behaviour of the coefficient of friction of thin films in micro-scale abrasion wear tests by rotative ball, the purpose of this work is to analyse the influence of the abrasive wear modes on the coefficient of friction of thin films in non-perforating tests, e.g., without reaching the substrates (like wear crater of Figure 2b-right).

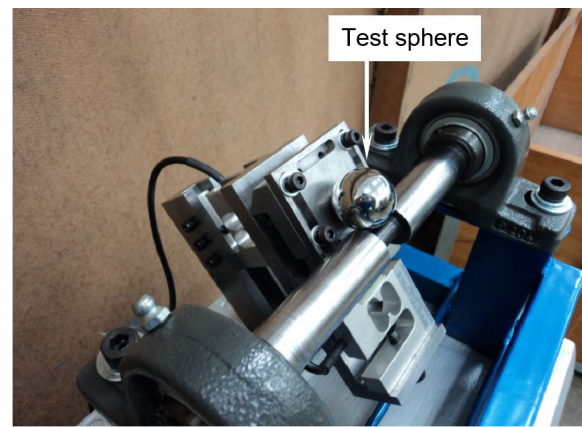


Figure 4. Ball-cratering micro-abrasive wear test equipment used in this work: free-ball mechanical configuration.

2 EQUIPMENT, MATERIALS AND METHODS

2.1 Micro-abrasive Wear Test Equipment

A ball-cratering equipment with free-ball configuration (Figure 4) was designed and constructed for the micro-abrasive wear tests.

Two load cells were used in the ball-cratering equipment: one load cell controlled the normal force (N) and one load cell measured the tangential force (T) that was developed during the experiments. The values of “ N ” and “ T ” are read by a readout system.

2.2 Materials

Experiments were conducted with thin films of TiN, CrN, TiAlN, ZrN, TiZrN, TiN/TiAlN, TiN/TiAlN (multi-layer), TiHfC and TiHfCN, with maximum thickness of $40\ \mu\text{m}$, deposited on substrates of cemented carbide. For the counter-body, one test sphere composed of AISI 52100 steel with a diameter of $D = 25.4\ \text{mm}$ ($D = 1''$) was used.

The abrasive material was black silicon carbide (SiC) with an average particle size of $3\ \mu\text{m}$. Figure 5 [12] presents a micrograph of the abrasive particles (Figure 5a) and its particle size distribution (Figure 5b). The abrasive slurries were prepared with SiC and glycerine.

2.3 Micro-abrasive Wear Tests

Table 1 presents the values of the test parameters defined for the experiments.

The normal force value defined for the wear experiments was $N = 0.4\ \text{N}$, with two abrasive slurries concentrations (C), $C_1 = 5\% \text{ SiC} + 95\% \text{ glycerin}$ and $C_2 = 50\% \text{ SiC} + 50\% \text{ glycerine}$ (volumetric values). These concentrations were designed to generate, respectively, “grooving abrasion” and “rolling abrasion” on the surface of the thin films. All tests were non-perforating, e.g., only the thin films were worn.

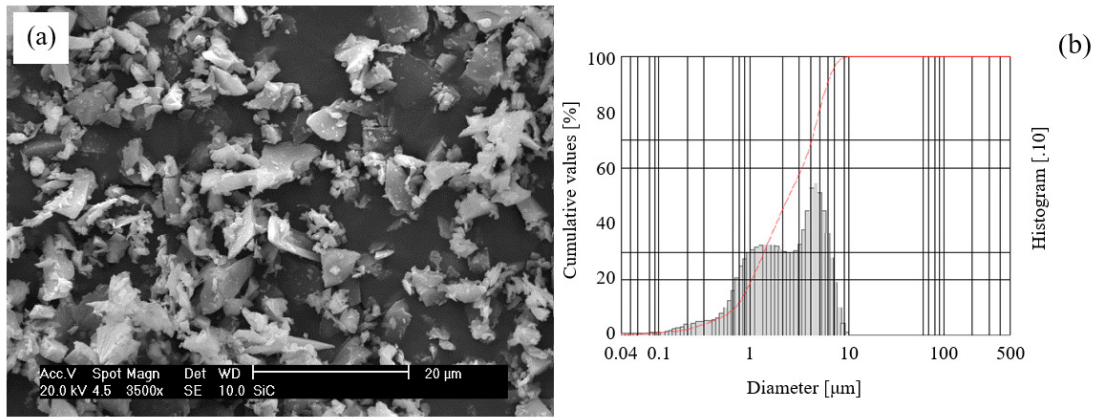


Figure 5. SiC abrasive [12]: (a) scanning electron micrograph and (b) particle size distribution.

Table 1. Test parameters selected for the ball-cratering wear experiments

Test parameter		Value
Normal force [N]	NI	0.4
Abrasive slurry concentration (in volume)	C_1	5% SiC + 95% glycerin
	C_2	50% SiC + 50% glycerin
Test sphere rotational speed [rpm]	n	70
Tangential sliding velocity of the test sphere [m/s]	v	0.09

The test sphere rotational speed was set to $n = 70$ rpm. With the value of $D = 25.4$ mm ($R = 12.7$ mm), the tangential sliding velocity of the test sphere was equal to $v = 0.09$ m/s.

The normal force (N) was constant during the tests; the tangential force (T) was monitored and registered during all experiments. The coefficient of friction (μ) was then calculated using Equation 7.

3 RESULTS AND DISCUSSION

For all thin films analysed in this work, Table 2 shows the values of the coefficient of friction (μ) as a function of the abrasive slurry concentration (C) and, consequently, as a function of the abrasive wear mode (“*grooving abrasion*” or “*rolling abrasion*”); the maximum error observed was $\mu = 0.11$. Additionally, for each thin film, there is the ratio between the terms $\mu_{Grooving}$ and $\mu_{Rolling}$, which are the coefficients of friction because of “*grooving abrasion*” and “*rolling abrasion*” abrasive wear modes, respectively.

For each thin film, the ratio $\frac{\mu_{Grooving}}{\mu_{Rolling}}$ was observed in two ranges: from $\frac{\mu_{Grooving}}{\mu_{Rolling}} = 1.13$ to $\frac{\mu_{Grooving}}{\mu_{Rolling}} = 1.46$ for the thin films of CrN, TiZrN, TiN/TiAlN, TiN/TiAlN (multi-layer), TiHfC and TiHfCN, and from $\frac{\mu_{Grooving}}{\mu_{Rolling}} = 2.25$ to $\frac{\mu_{Grooving}}{\mu_{Rolling}} = 2.71$ for the thin films of TiN, TiAlN and ZrN.

A significant increase in the volume of abrasive particles (from 5% SiC to 50% SiC) caused a decrease in the coefficient of friction.

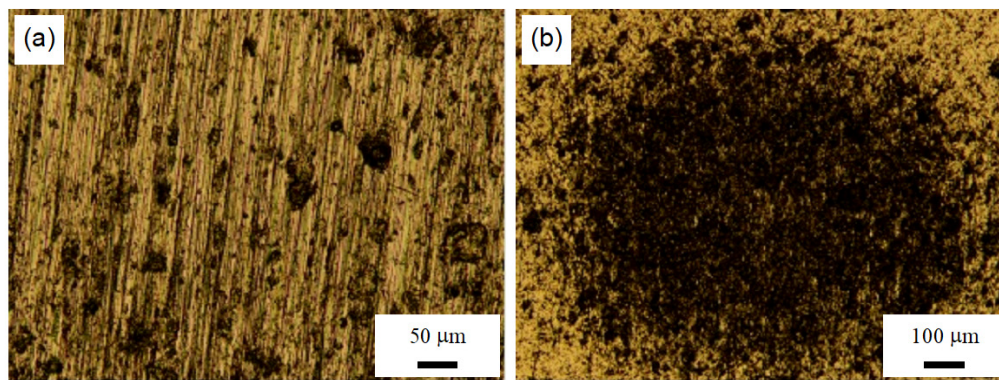
For each value of abrasive slurry concentration and, consequently, for each tribological condition of “*grooving abrasion*” or “*rolling abrasion*” abrasive wear mode, there were differences in the values of the coefficient of friction with respect to each thin film because the “coefficient of friction – μ ” is an intrinsic tribological characteristic of each material, which also depends of the test conditions and abrasive wear modes actions.

Figure 6 shows examples of wear craters obtained in the experiments; in all worn craters, the maximum depth (h) observed was approximately $h \approx 8$ μ m. Figure 6a displays the action of “*grooving abrasion*” characteristic of $C_1 = 5\%$ SiC + 95% glycerine. Figure 6b displays a wear crater under the action of “*rolling abrasion*”, reported for the abrasive slurry concentration $C_2 = 50\%$ SiC + 50% glycerine. These results qualitatively agree with the conclusions obtained by Trezona et al. [22], in which low concentrations of abrasive slurries (< 5% in volume of abrasive material, approximately) favour “*grooving abrasion*” and high concentrations of abrasive slurries (> 20% in volume of abrasive material, approximately) favour the action of “*rolling abrasion*”.

The abrasive slurry concentration and, consequently, the actions of the abrasive wear modes show an important influence on the coefficient of friction. The values of the coefficient of friction reported under “*grooving abrasion*”

Table 2. Coefficient of friction as a function of the abrasive slurry concentration (C) and abrasive wear mode (“*grooving abrasion*” or “*rolling abrasion*”)

Thin film	Coefficient of friction (μ)		
	$\mu_{Grooving}$	$\mu_{Rolling}$	$\frac{\mu_{Grooving}}{\mu_{Rolling}}$
	Grooving abrasion ($C_1 = 5\% \text{ SiC} + 95\% \text{ glycerin}$)	Rolling abrasion ($C_2 = 50\% \text{ SiC} + 50\% \text{ glycerin}$)	
TiN	1.37	0.57	2.40
CrN	0.35	0.24	1.46
TiAlN	0.72	0.32	2.25
ZrN	0.46	0.17	2.71
TiZrN	0.14	0.11	1.27
TiN/TiAlN	1.10	0.97	1.13
TiN/TiAlN (multi-layer)	1.23	0.87	1.41
TiHfC	1.67	1.20	1.39
TiHfCN	0.68	0.51	1.33

**Figure 6.** Occurrence of (a) “*grooving abrasion*” and (b) “*rolling abrasion*” on the surface of the thin films.

were higher than the values of the coefficient of friction reported under “*rolling abrasion*”.

This behaviour can be explained based on patterns of movements that act on “*grooving abrasion*” and “*rolling abrasion*”.

In “*grooving abrasion*”, the abrasive particles are fixed on the counter-body (in this case, on the ball), limiting their movements and requiring higher tangential forces. However, in “*rolling abrasion*”, the abrasive particles are free to roll between the ball and the specimen, facilitating the relative movement between these elements and consequently decreasing the coefficient of friction on the tribological system.

4 CONCLUSIONS

The results obtained in this work indicated the following:

- (1) The concentration of abrasive slurry affected the occurrence of “*grooving abrasion abrasive wear mode*” or “*rolling abrasion abrasive wear mode*”, as predicted by the literature [22];

- (2) With low concentration of abrasive slurry ($C_1 = 5\% \text{ SiC} + 95\% \text{ glycerine}$), the abrasive particles were incrustated on the counter-body (the test sphere), hindering their movements and generating high tangential forces. Thus, under this test condition, “*grooving abrasion abrasive wear mode*” has occurred and, consequently, high values of coefficient of friction were reported;

- (3) However, with high concentration of abrasive slurry ($C_2 = 50\% \text{ SiC} + 50\% \text{ glycerine}$) the abrasive particles were free to roll along the surface of the thin film. Consequently, in this case, “*rolling abrasion abrasive wear mode*” occurred, causing a low coefficient of friction.

Acknowledgements

The authors acknowledge CNPq – Brazilian National Research Council (Brasília-DF) for the financial support under process MCTI/CNPq – 482730/2012-9.

REFERENCES

- 1 Rutherford KL, Hutchings IM. Theory and application of a micro-scale abrasive wear test. *Journal of Testing and Evaluation – JTEVA*. 1997;25(2):250-260.
- 2 Cozza RC. A study on friction coefficient and wear coefficient of coated systems submitted to micro-scale abrasion tests. *Surface and Coatings Technology*. 2013;215:224-233.
- 3 Cozza RC, Tanaka DK, Souza RM. Friction coefficient and abrasive wear modes in ball-cratering tests conducted at constant normal force and constant pressure – Preliminary results. *Wear*. 2009;267:61-70.
- 4 Cozza RC, Rodrigues LC, Schön CG. Analysis of the micro-abrasive wear behavior of an iron aluminide alloy under ambient and high-temperature conditions. *Wear*. 2015;330-331:250-260.
- 5 Mergler YJ, Huis in 't Veld AJ. Micro-abrasive wear of semi-crystalline polymers. *Tribology and Interface Engineering Series*. 2003;41:165-173.
- 6 Cozza RC, Tanaka DK, Souza RM. Micro-abrasive wear of DC and pulsed DC titanium nitride thin films with different levels of film residual stresses. *Surface and Coatings Technology*. 2006;201:4242-4246.
- 7 Batista JCA, Godoy C, Matthews A. Micro-scale abrasive wear testing of duplex and non-duplex (single-layered) PVD (Ti,Al)N, TiN and Cr-N coatings. *Tribology International*. 2002;35:363-372.
- 8 Schiffmann KI, Bethke R, Kristen N. Analysis of perforating and non-perforating micro-scale abrasion tests on coated substrates. *Surface and Coatings Technology*. 2005;200:2348-2357.
- 9 Kusano Y, Van Acker K, Hutchings IM. Methods of data analysis for the micro-scale abrasion test on coated substrates. *Surface and Coatings Technology*. 2004;183:312-327.
- 10 Rutherford KL, Hutchings IM. A micro-abrasive wear test, with particular application to coated systems. *Surface and Coatings Technology*. 1996;79:231-239.
- 11 Cozza RC, Recco AAC, Tschiptschin AP, Souza RM, Tanaka DK. Análise comportamental dos coeficientes de atrito e desgaste de sistemas revestidos submetidos a desgaste micro-abrasivo. *Tecnologica em Metalurgia, Materiais e Mineração*. 2010;6(4):237-244.
- 12 Cozza RC. Influence of the normal force, abrasive slurry concentration and abrasive wear modes on the coefficient of friction in ball-cratering wear tests. *Tribology International*. 2014;70:52-62.
- 13 Neville A, Kollia-Rafailidi V. A comparison of boundary wear film formation on steel and a thermal sprayed Co/Cr/Mo coating under sliding conditions. *Wear*. 2002;252:227-239.
- 14 Dhanasekaran S, Gnanamoorthy R. Abrasive wear behavior of sintered steels prepared with MoS₂ addition. *Wear*. 2007;262:617-623.
- 15 Ceschini L, Palombarini G, Sambogna G, Firrao D, Scavino G, Ubertaini G. Friction and wear behaviour of sintered steels submitted to sliding and abrasion tests. *Tribology International*. 2006;39:748-755.
- 16 Shipway PH. A mechanical model for particle motion in the micro-scale abrasion wear test. *Wear*. 2004;257:984-991.
- 17 Kusano Y, Hutchings IM. Sources of variability in the free-ball micro-scale abrasion test. *Wear*. 2005;258:313-317.
- 18 Cozza RC. Estudo do desgaste e atrito em ensaios micro-abrasivos por esfera rotativa fixa em condições de “força normal constante” e “pressão constante” [tese]. São Paulo: Escola Politécnica da Universidade de São Paulo; 2011.
- 19 Cozza RC, Wilcken JTSL, Delijaicov S, Donato GHB. Tribological characterization of thin films based on residual stress, volume of wear, micro-abrasive wear modes and coefficient of friction. In: *Proceedings of the “ICMCTF 2017 – 44th International Conference on Metallurgical Coatings and Thin Films”*; 2017 Apr 24-28; San Diego – California, USA. San Diego: AVS – American Vacuum Society.
- 20 Cozza RC, Donato GHB. Study of the influence of the abrasive slurry concentration on the coefficient of friction of thin films submitted to micro-abrasive wear. In: *Proceedings of the “PacSurf 2016 – Pacific Rim Symposium on Surfaces, Coatings & Interfaces”*; 2016 Dec 11-15; 2016; Kohala Coast – Hawaii, USA. Kohala Coast: AVS – American Vacuum Society.
- 21 Cozza RC, Wilcken JTSL, Schon CG. Influence of abrasive wear modes on the volume of wear and coefficient of friction of thin films. In: *Proceedings of the “CoSI 2015 – 11th Coatings Science International”*; 2015 June 22-26; Noordwijk – The Netherlands. Noordwijk: Springer.
- 22 Trezona RI, Allsopp DN, Hutchings IM. Transitions between two-body and three-body abrasive wear: influence of test conditions in the microscale abrasive wear test. *Wear*. 1999;225-229:205-214.

Received: 13 July 2017

Accepted: 1 Jan. 2018